Neutron Diffraction Investigations of Magnetism in $BiFeO_3$ Epitaxial Films

William Ratcliff II, Daisuke Kan,* Wangchun Chen, Shannon Watson, Songxue Chi, Ross Erwin, Garry J. McIntyre, Sylvia C. Capelli, and Ichiro Takeuchi*

The recovery of a modulated magnetic structure in epitaxial $BiFeO_3$ thin films as revealed by neutron diffraction is reported. The magnetic structure in thin films is found to strongly depend on substrate orientation. The substrate orientation causes different strain–relaxation processes resulting in different thin-film crystal structures. The (110) oriented film with a monoclinic structural phase has a single-domain modulated magnetic structure where the magnetic moment lies in the HHL plane. For the (111) oriented film that has a rhombohedral structure, a modulated structure superimposed on the G-type antiferromagnetic order is found. These results indicate that slight structural modifications in the $BiFeO_3$ thin film cause drastic changes in the magnetic structure.

1. Introduction

Multiferroics are materials that exhibit both magnetic and ferroelectric order parameters. Recent years have seen a renaissance in the study of these materials, resulting in the discovery of many new materials in which the magnetic and ferroelectric order parameters are coupled. However, for most of these materials, the ordering temperatures are far too low for device applications. Perovskite-structured $BiFeO_3$ (BFO) with a rhombohedral distortion along the [111] direction (space group R3c) is a rare exception to this trend, with a ferroelectric transition temperature T_c of 820 °C[1] and an antiferromagnetic transition temperature T_N of 370 °C.[2] It has been demonstrated that an applied electric field can effect the magnetic domain population in BFO thin films[3].

Dr. W. Ratcliff II, Dr. W. Chen, Dr. S. Watson, Dr. S. Chi, Dr. R. Erwin
100 Bureau Drive
MS 6102, NIST Center Neutron Research
NCNR, 100 Bureau Drive, Gaithersburg, Maryland 20899, USA
E-mail: william.ratcliff@nist.gov
Dr. D. Kan,[+] Prof. I. Takeuchi
Department of Materials Science and Engineering
University of Maryland
College Park, Maryland 20742, USA
Dr. G. J. McIntyre, Dr. S. C. Capelli
Institut Laue-Langevin
BP 156, 38042 Grenoble Cedex 9, France
[+] Current address: Institute for Chemical Research, Kyoto University, Uji, Kyoto, 611–0011, Japan; E-mail: dkan@scl.kyoto-u.ac.jp

DOI: 10.1002/adfm.201002125

The study of the magnetic structure of bulk BFO started with powders and evolved to single crystals when large ones became available. These single-crystal studies definitively showed that the magnetic structure in the bulk was a long-wavelength spiral[4] in the plane which contains one of the ferroelectric polarization and the propagation vector. The rhombohedral crystallographic symmetry results in a degeneracy in the free energy, giving rise to the possibility of magnetic domains. Each possible magnetic domain is characterized by one of three equivalent propagation vectors (related by rotations about the 3 fold axis): $\vec{k_1} = [\partial 0 \bar{\partial}], \vec{k_2} = [0 \partial \bar{\partial}]$, $\vec{k_3} = [\bar{\partial} \partial 0]$, with $\partial = 0.0045$, which corresponds to a periodicity of 620 Å. [4] Remarkably, as-grown bulk crystals form with only a single ferroelectric and a single magnetic domain. Furthermore, associated with each propagation vector, there is the possibility that the spiral could be either left or right handed. However, the spirals in the bulk were found to possess a single chirality.[4]

However, there have not been similarly detailed studies of the magnetic structure in thin film samples. Such work is critically important, as the multiferroic properties of BFO are likely to be highly dependent on the changes in strain that accompany the transition from bulk crystal to thin film geometry. One recent study[5] has shown that the spiral as observed in the bulk is not present in the thin film. This means that the long-wavelength spiral observed in the bulk collapses to a G-type antiferromagnetic order in which the Fe magnetic moments are coupled ferromagnetically in the (111) planes and antiferromagnetically between adjacent planes, leading to the doubling of the magnetic unit cell in all crystallographic directions from the nuclear unit cell.[22] This is manifested as a single peak at the (0.5 0.5 0.5) position in reciprocal space. However the detailed magnetic structure in the thin film form of BFO still remains unclear.

In this paper, we investigate how the thin film geometry affects the magnetic structure of BFO. To this end, we pursued a neutron diffraction study of the magnetic structure of BFO epitaxial films grown on $SrTiO_3$ (STO) substrates with various orientations. Our unpolarized and polarized neutron diffraction studies reveal that the film has a different magnetic structure depending on the substrate orientation. For the (110) oriented film with the monoclinic M_b structural phase, the magnetic structure is found to be a single-domain modulated magnetic structure where the magnetic moment lies in the HHL plane.

The (111) oriented film, in which the rhombohedral structure is maintained, has a modulated structure superimposed on the G-type order. These results indicate that the magnetic structure of BFO thin films is susceptible to subtle changes in its crystal structure resulting from the different epitaxial strain relaxation process dependent upon the substrate orientation.

2. Experimental Results and Discussions

Due to the rhombohedral distortion along the [111] direction, epitaxially-grown $BiFeO_3$ thin films have crystallographic domain structures depending on substrate orientations. The (001) oriented film, for instance, has four equivalent [111] crystallographic directions, creating four crystallographic domain structures. However, this multiple crystallographic domain structure makes determination of the magnetic structure complex, since the multiple magnetic domain structures could form even in a single crystallographic domain due to a six-fold degeneracy for the orientation of the magnetic moment within a given (111) plane.[3,6] To minimize this complexity, we have chosen thin films grown on (110) and (111) STO substrates in which a (quasi-) single crystallographic domain structure can be achieved as confirmed in **Figure 1**. The BFO films studied here have been fabricated by pulsed laser deposition with a thickness of 1 μm in order to minimize the strain effect which could modify the magnetic structure in BFO.[7] Our recent X-ray diffraction study[8] confirms that the fabricated BFO films have different structures depending on the substrate orientations even if the film thickness exceeds the critical thickness of ~100 nm,[9,10] at which BFO thin films begin to relax from the epitaxial strain induced by the substrate. For the (110)-oriented film, the crystal structure is found to be a monoclinic structure, the so-called M_b phase.[8,11] The lattice parameters are determined to be $a_m = 5.645$ Å, $b_m = 5.589$ Å, $c_m = 3.950$ Å and $\beta = 90.85°$ (The subscript m denotes monoclinic). In the reciprocal-space-maps (RSMs) shown in Figure 1a and b, we see two reflections corresponding to two crystallographic domains in the film. However, it should be noted that one reflection has an intensity more than twenty times larger than the other. (The intensity ratio slightly depends on the reflection index.) Therefore the contribution from the minor domain is negligible and the film can be regarded as having a quasi single-crystallographic domain. In the case of the (111)-oriented film, a single crystallographic domain structure with rhombohedral symmetry is found to be maintained and the lattice parameters are determined to be $a = 3.968$ Å and $\alpha = 89.4$. These lattice parameters are in good agreement with the lattice parameters in bulk.[12] Figure 1c shows a RSM around the STO (132) Bragg reflection taken for a (111)-oriented thin film. The observed single reflection from the BFO layer indicates that the no twin crystallographic domain is formed along the [–110] direction. We note that around the (114) Bragg reflection (along the [11–2] direction) there is also only a single reflection observed (not shown). These observations reveal that the (111) film is a single crystallographic domain. Ferroelectric properties for the fabricated BFO films are confirmed by room-temperature square-shaped ferroelectric hysteresis loops as seen in Figure 1d. The observed saturated ferroelectric polarizations are ~85 and

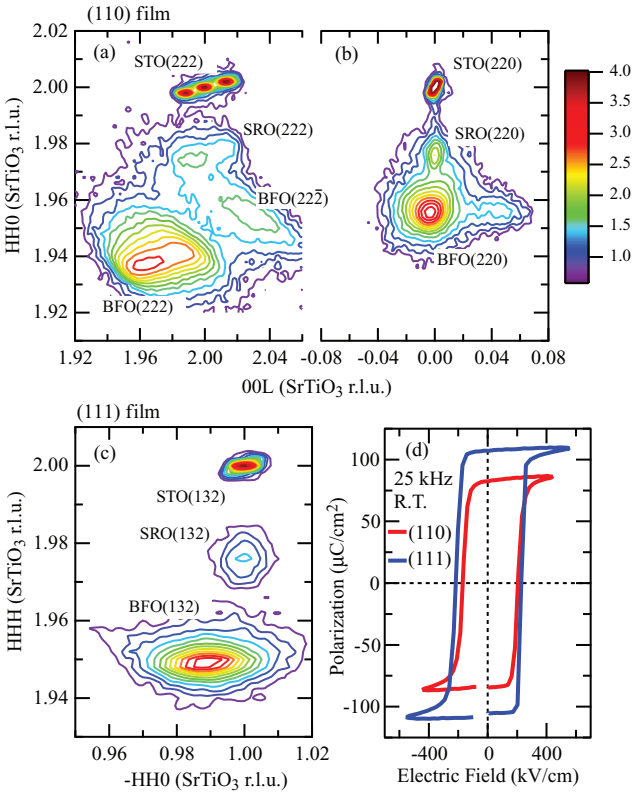

Figure 1. Structural and ferroelectric properties for (110) and (111) oriented $BiFeO_3$ thin films. a–c) show semi-logarithmic contour plots of the X-ray reciprocal space mappings taken for 1μm-thick $BiFeO_3$ (BFO) films grown on $SrTiO_3$ (STO) substrates with (110) and (111) orientations. The mappings in (a) and (b) were taken for the (110) film around the STO (222) and (220) Bragg reflections, respectively. Note that the splitting in reflection intensity was observed only along the [001] direction. The two reflections observed from the BFO layer indicate that two crystallographic domains exist in the film. Based on the reflection intensity ratio, the population of one of the domains is negligibly small. In (c), the scans were performed with the (111) oriented film around the STO (132) Bragg reflection, exhibiting a single reflection from BFO layer. This confirms that the (111)-oriented film has the single crystallographic domain structure. In (a –c), STO, SRO, and BFO denote $SrTiO_3$, $SrRuO_3$, and $BiFeO_3$, respectively. The mappings are plotted in units of the reciprocal lattice unit of STO. d) Room-temperature polarization hysteresis loops for the (110) and (111) oriented films. The loops were measured at 25 kHz.

~110 μC cm^{-2} for the (110) and (111)-oriented film, respectively. These values are in good agreement with the value predicted by the projection rule.[13]

We used neutron scattering to probe the magnetic structures of the films. The equation for the differential cross section describing the coherent elastic scattering of neutrons from magnetically ordered crystals in the ground state is given by:[14–16]

$$\frac{d\sigma}{d\omega} \propto N_M \frac{2\pi^3}{V_M} \sum_{\vec{G}_M} \delta(\vec{Q} - \vec{G}_M) |\vec{F}_M(\vec{G}_M)|^2 \quad (1)$$

where N_M is the number of magnetic unit cells in the crystal and V_M denotes the volume of the magnetic unit cell. The magnetic structure factor $\vec{F}_M$ is defined by:

$$\vec{F}_M(G) = \left(\frac{\gamma\mu_0 e^2}{4\pi m_e}\right)^2 \left\langle 1 - \left(\hat{G}\cdot\hat{M}\right)^2 \right\rangle \sum_{j=1}^{N} \langle\vec{\mu}_j\rangle f_j(G)\, e^{iG\cdot r_j}\, e^{-W} \quad (2)$$

where the neutron-electron coupling constant in parentheses is -0.27×10^{-14} m, $\hat{G}$ and $\hat{M}$ are unit vectors in the direction of the reciprocal lattice vector $\vec{G}$ and the average moment direction. Here $\langle\vec{\mu}_j\rangle$ is the thermal average of the ordered magnetic moment of the j^{th} atom in the unit cell, r_j is the position of the j^{th} atom in the magnetic unit cell, $f_j(\vec{Q})$ is the scalar magnetic form factor of the j^{th} atom in the cell, and the sum j ranges over all atoms in the unit cell. The (scalar) magnetic form factor is the Fourier transform of the magnetization density associated with each atom. An important consequence of the factor in triangular brackets in (2) is that the observed cross section is only sensitive to the component of the moment in the plane perpendicular to the measured reflection.

We shall start our discussion with neutron diffraction measurements of the 1 µm-thick film grown on a (110) oriented STO substrate. Due to the close lattice constants of STO (a = 3.905Å) and BFO (a = 3.96Å, α = 89.4° in buk) and the relatively weak signal from the film relative to the substrate, the orientation of the film and all measurements are given in units of the STO lattice constants. In **Figure 2**a, we show a reciprocal space mapping of the HHL zone of the film. The measurements were performed at room temperature in the reciprocal spaces around (0.5 0.5 0.5) where the observed neutron signal should arise from the magnetic order present in the BFO film, as the STO has no magnetic order and shows only the nuclear reflections. If the spiral structure existed as observed in the bulk form, we would expect multiple peaks in the reciprocal space around (0.5 0.5 0.5)[4] as the G-type antiferromagnetism gives way to a spiral structure with propagation vector $[\partial 0\bar{\partial}]$ as discussed earlier.

As one can see in Figure 2a, our fabricated (110) film clearly exhibits two reflections in the scattering zone. The spacing between two peaks is 0.0053(1) reciprocal lattice units (rlu) which is consistent with the bulk spin modulation period of 620 Å. Given that the relative intensities of the two reflections is similar, it is unlikely that they come from two separate crystallographic domains since the X-ray RSMs in Figure 1a and b show that this film, while having two twins present, is dominated by one twin domain. Thus, we can see that a modulated structure is achieved in (1 1 0) oriented films. Importantly, these reflections are consistent with a propagation vector along the [1 1 –2] direction rather than the [1 0 –1] direction found in the bulk. The direction of the propagation vector was identified from fits of the observed intensity to two dimensional gaussians to determine the centers of the reflections. These centers were then used to determine the propagation vector of $[\partial\partial 2\bar{\partial}]$. This direction was also confirmed by measuring the scattering angle of the observed reflections to confirm that they were satellites of the (0.5 0.5 0.5) reflection rather than a (0.5 0.5 –0.5) reflection. Given the positions, they are not coming from possible other magnetic domains with a propagation vector along the <1 1 0> family of directions being projected into the scattering plane. Furthermore, the relatively weak film (1 1 0) reflection was found and a measurement was performed in that reference system to verify the propagation vector. For further testing, offsets were intentionally introduced to the instrument angles to determine if instrumental error could explain the position of the reflections. All observations were consistent and can only be explained by a propagation vector of $[\partial\partial 2\bar{\partial}]$.

To examine possible formation of magnetic domains in the film, we show a cartoon of the relative positions of reflections in the HHL zone from all possible magnetic domains with a propagation vector along a family of the [11–2] direction in Figure 2b. These domains would arise from rotations about the three fold axis and would result in [1 –2 1] and [–2 1 1] propagation vectors. In the HHL zone (Figure 2a), if magnetic domains are present, they will be out of the scattering plane; however, due to the broad vertical resolution of the triple-axis-spectrometer, they would be detected in the scattering plane as found in previous neutron studies on bulk single crystals.[17] However,

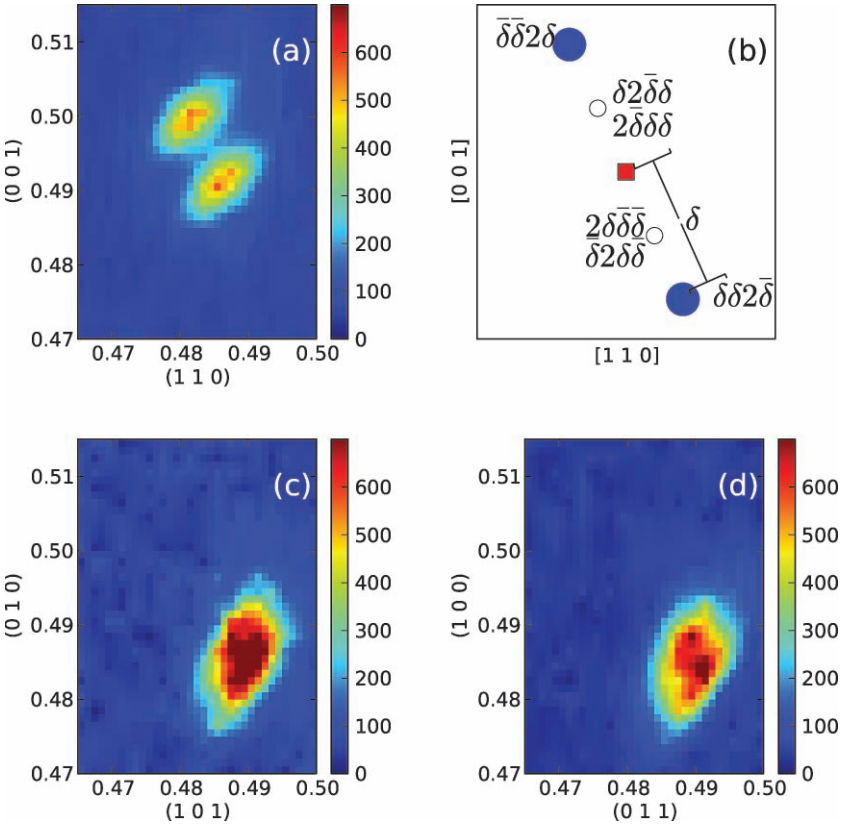

Figure 2. Unpolarized neutron diffraction for the 1 µm-thick (110) oriented $BiFeO_3$ film. a,c,d) Reciprocal space maps taken in HHL, HKK, and HKH zones, respectively. b) A cartoon showing the relative positions of reflections from different magnetic domains. Blue circles lie in the scattering plane. White circles represent the projection of reflections into the HHL scattering plane. The cartoon is centered about a reflection of (0.5 0.5 0.5) shown as a red square.

in Figure 2a there is no indication of contribution from these other domains (which would be reflected in intensity present at the (0.5 0.5 0.5) ± ($\frac{\delta}{2}$ $\frac{\delta}{2}$ 0) positions) implying that the film has a single magnetic domain. To more fully investigate this point, we examined several different scattering zones. Representative meshes are shown in Figure 2c and d for the HKH, and HKK zones, respectively. For both measured zones, a single peak is clearly observed. If multiple domains were present, instead of seeing a single reflection, we would expect to see multiple reflections in another zone in which both satellites were separated. Thus, we conclude that this film consists of a single magnetic domain.

Another reasonable question to ask is whether the observed two reflections arise from a modulation in the angle between the adjacent magnetic moments or the amplitude of magnetic moment, namely a spiral or an amplitude modulated magnetic structure. To address this, we turn to polarized neutron measurements. In polarized neutron diffraction, the neutron spin state is selected prior to scattering by the sample. After scattering from the sample, the spin of the outgoing neutron is measured. We measure in the channels in which the neutron spin is flipped, or not flipped by interaction with the sample. Neglecting incoherent scattering, the canonical equations governing polarized neutron diffraction are given by:[17]

$$\begin{aligned}
\frac{d^2\sigma^{++}}{d\Omega d\omega} &= \frac{k_f}{k_i}[\langle NN^*\rangle_\omega + \hat{P}\cdot\langle N\overrightarrow{M_\perp^*}\rangle_\omega \\
&\quad + \hat{P}\cdot\langle N^*\overrightarrow{M_\perp}\rangle_\omega + \langle(\hat{P}\cdot\overrightarrow{M_\perp})(\hat{P}\cdot\overrightarrow{M_\perp^*})\rangle_\omega] \\
\frac{d^2\sigma^{--}}{d\Omega d\omega} &= \frac{k_f}{k_i}[\langle NN^*\rangle_\omega - \hat{P}\cdot\langle N\overrightarrow{M_\perp^*}\rangle_\omega \\
&\quad - \hat{P}\cdot\langle N^*\overrightarrow{M_\perp}\rangle_\omega + \langle(\hat{P}\cdot\overrightarrow{M_\perp})(\hat{P}\cdot\overrightarrow{M_\perp^*})\rangle_\omega] \\
\frac{d^2\sigma^{+-}}{d\Omega d\omega} &= \frac{k_f}{k_i}[\langle\overrightarrow{M_\perp}\overrightarrow{M_\perp^*}\rangle_\omega - \langle(\hat{P}\cdot\overrightarrow{M_\perp})(\hat{P}\cdot\overrightarrow{M_\perp^*})\rangle_\omega \\
&\quad - i\langle(\hat{P}\cdot(\overrightarrow{M_\perp}\wedge\overrightarrow{M_\perp^*})\rangle_\omega] \\
\frac{d^2\sigma^{-+}}{d\Omega d\omega} &= \frac{k_f}{k_i}[\langle\overrightarrow{M_\perp}\overrightarrow{M_\perp^*}\rangle_\omega \\
&\quad - \langle(\hat{P}\cdot\overrightarrow{M_\perp})(\hat{P}\cdot\overrightarrow{M_\perp^*})\rangle_\omega + i\langle(\hat{P}\cdot(\overrightarrow{M_\perp}\wedge\overrightarrow{M_\perp^*})\rangle_\omega]
\end{aligned} \tag{3}$$

In these equations, k_f and k_i are the outgoing and incoming wave-vectors of the neutron respectively. P is the polarization of the neutron and M is the moment direction in the sample. N denotes nuclear scattering. Plus and minus indicate the polarization state of the neutron. Essentially, these equations show that spin flip (SF) scattering, in which the spin of the neutron is flipped by interaction with the sample, is sensitive to the components of the sample's magnetic moment perpendicular to the polarization of the neutron and that non spin flip (NSF) scattering is sensitive to the components of the sample's moment parallel to the polarization of the neutron. This is schematically shown in **Figure 3**.

For the polarized beam measurement, we focused on the two magnetic reflections observed in the reciprocal space around (0.5 0.5 0.5) in the HHL zone. **Figure 4**a shows the scattering geometry for the measurements. In Figure 4b, we show measurements of SF and NSF scattering with the neutron polarization

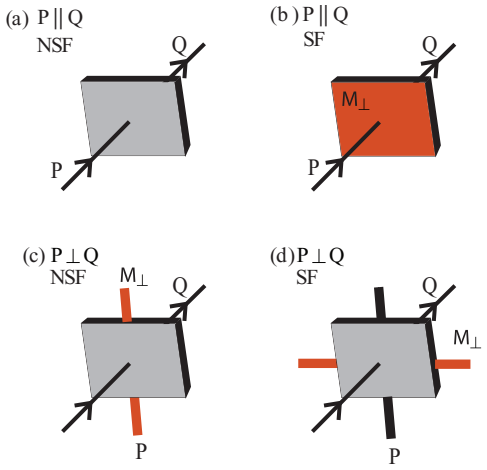

Figure 3. A cartoon of polarized neutron diffraction. The neutron polarization is either in the scattering plane, or is normal to it. The neutron is sensitive to the component of the magnetic moment of the sample normal to the scattering wave vector, Q which lies in the scattering plane. We denote this component by $M_\perp$. Red indicates the directions of the electron moment to which the neutron will be sensitive. a) The neutron polarization, P, is parallel to Q and we consider non spin flip (NSF) scattering. Here, we are not sensitive to the electron moment at all as discussed in the text. b) The neutron polarization is parallel to Q and we consider spin flip (SF) scattering. Here, the neutron is sensitive to moments in the red plane. c) We consider the case of the neutron polarization perpendicular to the scattering plane. In the NSF channel, the cross section is sensitive to the projection of the electron moment along the direction in which the neutron is polarized, shown in red. d) In the SF channel, with the neutron polarization perpendicular to the scattering plane, the cross section is sensitive to the projection of the moment along the red line shown in the figure. We remind the reader that the grey plane shown is not necessarily the plane of the film, but is an abstract plane which is normal to the scattering wave vector, Q.

parallel to the scattering vector, Q. In this figure, we see that SF scattering dominates NSF (the offset in backgrounds is due to incoherent scattering and the presence of weak NSF scattering is due to incomplete polarization of the incident beam). This tells us that the magnetic moment is normal to the scattering vector of (0.5 0.5 0.5) and is thus either out of the scattering plane, or along the [1 1 –2] direction in the scattering plane, although we are not sensitive to components of the moment along the [111] direction. Thus, Figure 4b tells us that we have magnetic scattering, but does not limit the direction. In Figure 4c we show measurements of SF and NSF scattering with the neutron polarization out of the scattering plane. Again, we see that SF scattering is dominant over NSF scattering. This leads to the conclusion that the moment has a component along the [1 1 –2] direction, which is one of the axes in the hexagonal unit (with some possible component along the [111] direction) cell of BFO. To check this further, we rotated the neutron polarization within the scattering plane and observed how the intensity changes. In Figure 4d, we show how the intensity (of the right peak from Figure 4b) varies with the angle of the sample guide field rotation. An angle ~ 0 degrees corresponds to polarization along the scattering vector. The intensities have been corrected for spatial inhomogeneity in the spin transport using the flipping ratio of a nuclear peak measured over the same range. From this, we can see that there is variation and that the NSF

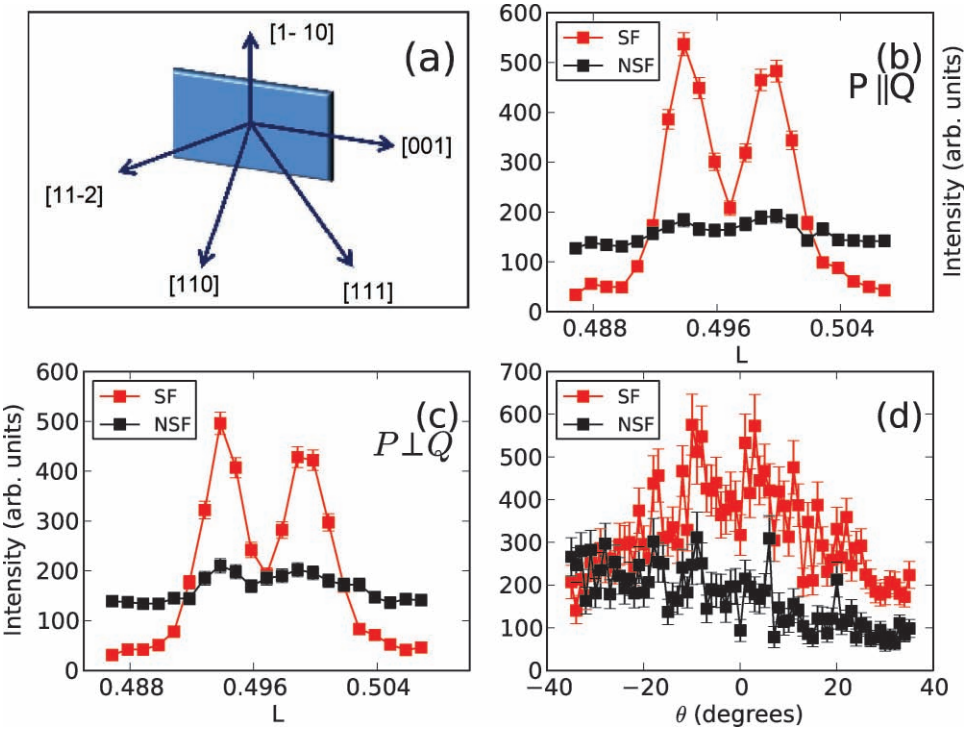

Figure 4. Polarized diffraction measurements of the (110) oriented $BiFeO_3$ film. a) Cartoon of the scattering geometry for the measurements. b,c) Intensity profiles taken in HHL zone with (b) *P*(neutron polarization)//*Q*(scattering vector) and (c) *P*⊥*Q*. d) Changes in scattering intensites with the polarization rotated by an angle θ (measured in degrees) within the scattering plane relative to the scattering wave vector (that is, an angle of 0 corresponds to the neutron polarization along the scattering wavevector) In (b–d), the red and black squares represent spin-flip (SF) and non spin-flip (NSF) scattering, respectively. The data have been corrected for spin transport as described in the text. Error bars where indicated are statistical in origin and represent one standard deviation.

channel also shows variation. This is all consistent with a magnetic moment with a component along the hexagonal axes (the [1 1 –2] direction in the pseudo-cubic notation) with some component possibly along the [111] direction. Thus we conclude that in the (110) oriented film, we have a single domain, modulated magnetic structure although we are not able to resolve whether the magnetic structure is a spiral, or a modulated structure, due to our lack of sensitivity to a component of the moment along the [111] direction. However, we are able to restrict the moment to the HHL plane.

Next, we turn to the film grown on the (111) oriented STO substrate, where a single crystallographic domain with rhombohedral symmetry is maintained.[8] As with the (110) oriented film, we start our investigations with unpolarized beam measurements. **Figure 5** shows a RSM around (0.5 0.5 0.5) in HHL scattering zones. We see a rather broad peak, which is broader than the instrumental resolution. Note, in contrast to the (110) film, there are no well-separated reflections observed in contrast to the (110) film case in Figure 2a. We also examined several different scattering zones of the film. Figures 5b and c show the representative results for RSMs taken in HKK and HKH zones, respectively. Clearly there is a single broad peak present in both measured zones. Thus, from the unpolarized beam measurements, it is hard to make any conclusions about the nature of the magnetic structure. Thus again, we turn to polarized beam measurements.

This time, we orient the film in the (H K (H+K)/2) scattering plane, which is defined by the (1 1 1) and (1 –1 0) reflections as shown in **Figure 6**a. In Figure 6b we show SF and NSF measurements on the magnetic reflection around (0.5 0.5 0.5) with the neutron polarization *P* parallel to the scattering vector *Q*. A single peak is clearly observed for both SF and NSF configurations, indicating that there is a (0.5 0.5 0.5) ordering wave vector present. In Figure 6c, we show SF and NSF measurements performed with *P* out of the scattering plane. Here, we notice that now NSF scattering dominates SF scattering. Furthermore, we note that there are clearly two peaks present in the SF channel. As we only can observe a separation of the peaks in the SF channel with *P* normal to the scattering plane, this means that the moment associated [0.5 0.5 0.5] G-type ordering wave vector has a component along the [1 1 –2] direction so as to obscure the separation seen in the SF vertical neutron polarization channel. As we are insensitive to the component of the moment along the [111] direction, this places the moment for this G-type order in the HHL plane. This is the reason for the (0.5 0.5 0.5) broad peak observed in the unpolarized beam experiments—there is a modulated structure superimposed upon the magnetic G-type ordering for the (111) film (Figure 5). In Figure 6d we again investigated the variation of the intensity with the angle of the in-plane neutron polarization. The flat nature of the curve reveals that the G-type ordering peak dominates the signal with its moment having a strong component along the [1 1 –2] direction.

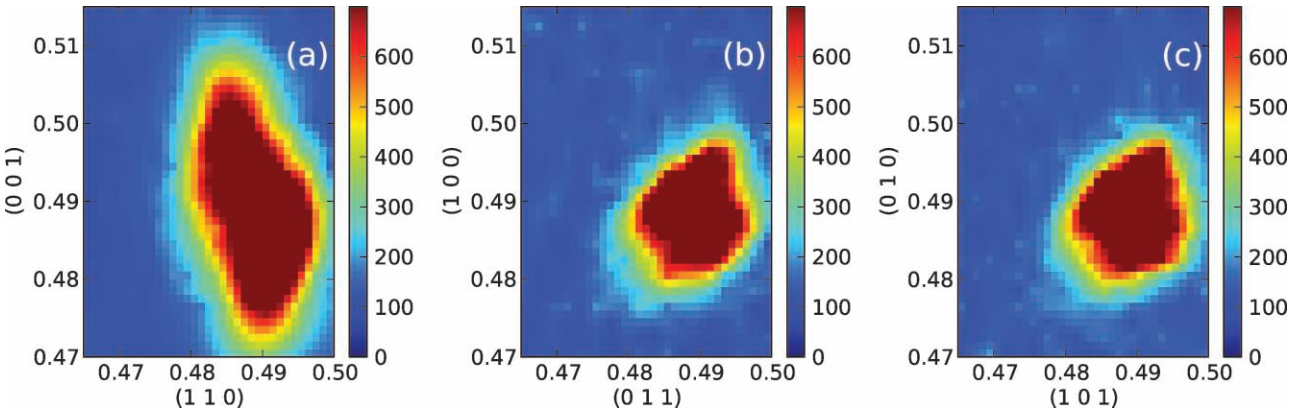

Figure 5. Unpolarized neutron diffraction for the 1 μm-thick (111) oriented $BiFeO_3$ film. The reciprocal space mappings were taken in the a) HHL, b) HKK and c) HKH zones.

Unfortunately, we can say relatively little about the modulated structure for the (111) film. However, one thing which is clear from the observations in Figure 6c is that the modulated magnetic moment is comparable in magnitude to the G-type ordering, and has a strong component along [1 –1 0], lying within the plane containing [1 -1 0] and [1 1 1]. Finally, we note that despite looking for evidence of chirality by distinguishing the +– channel from the –+ channel, we could not observe any asymmetry. However, this may simply be due to the presence of chirality domains in the film that were not present in the bulk.

Our observations have demonstrated that it is possible to recover a modulated structure in the thin films. Examples of possible modulated magnetic structures consistent with our observations are shown in **Figure 7**. In addition, we have found that the substrate orientation, which results in different strain relaxation processes leading to the different thin-film structural phase,[8] has a bearing on the magnetic structure in the film. Our preliminary neutron diffraction studies for the (001) oriented film shows that there is only a single reflection around (0.5 0.5 0.5), revealing that the magnetic structure of the (001)

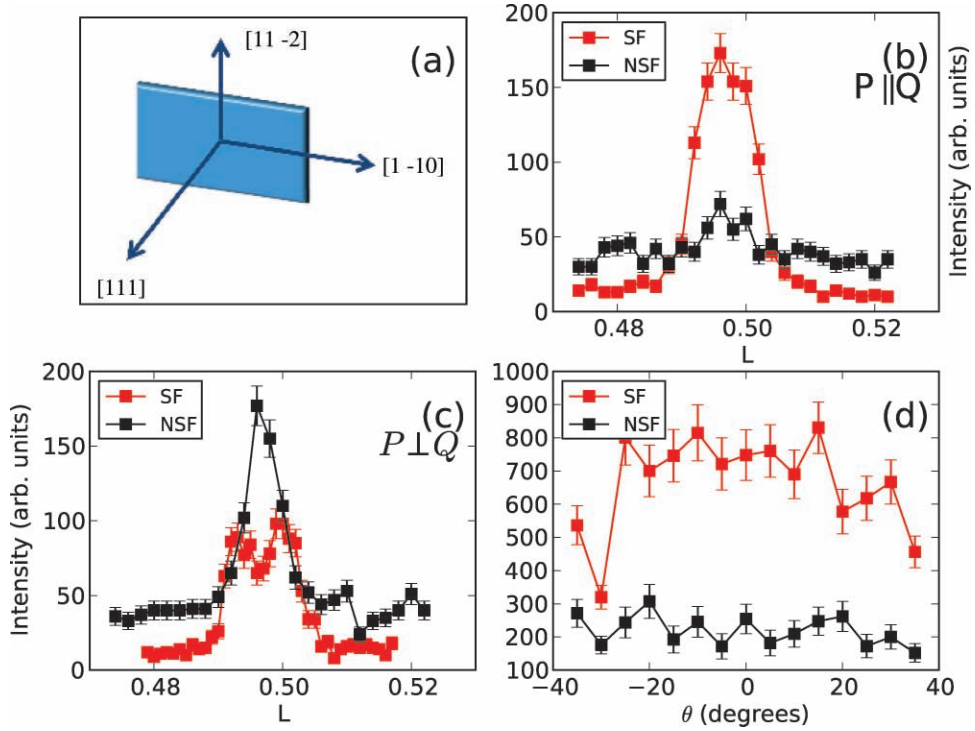

Figure 6. Polarized diffraction measurements of the (111) oriented $BiFeO_3$ film. a) Cartoon of the scattering geometry for the measurements. b,c) Intensity profiles taken with (b) P(neutron polarization)//Q(scattering vector) and (c) $P \perp Q$. d) Changes in scattering intensities with the polarization rotated by an angle θ (measured in degrees) within the scattering plane relative to the scattering wave vector (that is, an angle of 0 corresponds to the neutron polarization along the scattering wavevector) In (b–d), the red and black squares represent spin-flip (SF) and non spin-flip (NSF) scattering, respectively. The data have been corrected for spin transport as described in the text.

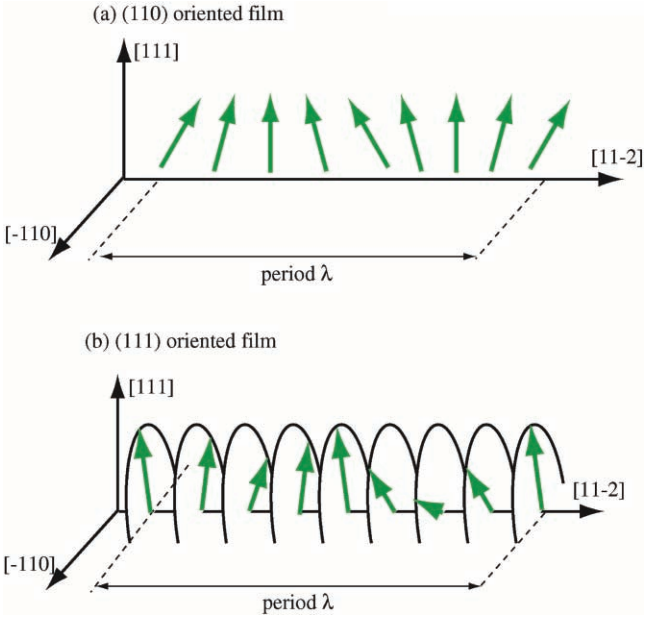

Figure 7. Cartoon of possible magnetic structures for (110) and (111) oriented $BiFeO_3$ thin films. a) A possible magnetic structure for (110) film where the magnetic moments lies in the HHL plane containing the [111] and [11–2] directions. The propagation vector is along the [11–2] direction. b) A possible magnetic structure for the (111) film where the G-type ordering occurs in the plane containing the [111] and [11–2] directions, and the modulated components appears along the [–110] direction with the propagation vector is along the [11–2] direction.

oriented film is G-type antiferromagnetic structure (see Supporting Information). However, for the (110) oriented film, a single domain, modulated magnetic structure is observed in which spins lie in the HHL plane. The propagation vector associated with this order is different from that found in the bulk. For the (111) oriented film, a modulated structure is observed, but the G-type order is also present. It is interesting to point out that the structural symmetry for the (001) and (110) oriented film has been lowered to the monoclinic M_a and M_b phase, respectively[8]. This symmetry-lowered structural phase could lift the degeneracy in the easy magnetization axis and change the ground state for the magnetic structure. This could be a reason for the single-domain modulated magnetic structure observed in the (110) film. Recent first-principles calculations[3] also suggest that the monoclinic distortion may be the reason for creating the easy magnetization axis in BFO. This also supports our experimental observations.

Another implication of our observation is the possibility of growing magnetoelectric devices in film form based on the spiral magnetic structure. The recent work of Lebeugle et al.[18] has shown that it is possible to electrically switch the easy magnetization axes of permalloy deposited on single crystals of BFO. They suggest that the mechanism is strongly related to the presence of the spiral. We have shown that changing the film growth orientation is sufficient to re-establish a modulated magnetic structure in BFO thin films. Further work needs to be done to determine whether the modulation comes from a spiral or an amplitude modulated structure. If it turns out that the structure is a spiral as in the bulk, we should be able to exploit the same mechanism for device applications. Even if the magnetic structure is amplitude-modulated, it still opens the possibility of novel device applications. The electric field induced magnetization switching of exchanged coupled Co layer on a (001) oriented BFO film previously reported[19] points to a mechanism other than one involving the spiral. The implication of this to the present observation is that the ferroelectric domains in BFO films could couple to the amplitude-modulated antiferromagnetic domains and that this coupling mechanism can be utilized for thin film device applications.

3. Conclusions

We have shown that is possible to recover a modulated magnetic structure in epitaxial $BiFeO_3$ thin films. Furthermore, we have found that the magnetic structure strongly depends on the substrate orientation of the film. For the (001) oriented substrate, we found that there was only commensurate G-type antiferromagnetism present even for films as thick as 1 μm. Whereas, 1 μm-thick films grown on (110) and (111) oriented STO substrates evinced modulated magnetic structures. In the (110) film, we found a single magnetic domain with a modulated structure, whereas both G-type and modulated magnetic structures were found in the (111) oriented film. The recovery of a modulated magnetic structure in thin films opens the door to novel coupling between BFO films and magnetic layers deposited on top of them.

4. Experimental Section

$BiFeO_3$ thin films with thicknesses up to 1 μm were grown epitaxially on (001), (110), and (111) oriented $SrRuO_3$-buffered $SrTiO_3$ substrates by pulsed laser deposition. During the deposition, the substrate temperature and oxygen pressure were kept at 590 °C and 25 mTorr (3.33 Pa). For structural characterization, a conventional 4-circle XRD (Bruker D8)[20] was used. Ferroelectric properties were characterized with a Radiant Premiere II[20] loop analyzer at room temperature.

Unpolarized and polarized neutron diffraction measurements were performed respectively on the BT9 and BT7 thermal triple-axis instruments at the NIST Center for Neutron Research. The measurements performed on BT9 used relatively tight Söller collimations of 40′-11′-S-40′-120′ full-width-at-half maximum (FWHM). We placed PG filters both before and after the sample to suppress higher order wavelengths. For the polarized beam measurements performed on BT7, we used slightly more relaxed Söller collimations of 50′-25′-S-50′-open FWHM. Polarization was achieved through the use of ^3He cells[21] placed before and after the sample. Flipping ratios as high as 10 were achieved initially. However, as the polarizion of the cell decays with time, flipping ratios lowered with time. Cells were replaced during the experiment to maintain acceptible flipping ratios. Measurements presented in the figures are close enough in time that corrections for the lowered polarization of the cell are unnecesary. All measurements were done at room temperature. Measurements on a BFO film grown on (0 0 1)-oriented STO were also performed on the D10 four-circle diffractometer at the ILL (Grenoble, France), in a beam of wavelength 2.359 Å from a PG [0 0 2] monochromator on a thermal neutron guide. A PG filter was placed before the sample to suppress higher-order contaminations. The resolution at focusing was 20'. Data were collected with a position sensitive detector with pixel spacing equivalent to 12' in both directions, but the true resolution was dominated by the dimensions of the substrate face and the 1.7° vertical focusing of the monochromator.

Supporting Information

Supporting Information is available from the Wiley Online Library or from the author.

Acknowledgements

We would like to acknowledge useful discussions with Dr. J. Borchers. Work at Maryland was supported by access to the Shared Experimental Facilities of the UMD-NSF-MRSEC (DMR 0520471), NSF DMR 0603644, and ARO W911NF-07–1-0410. The work was also supported by the W. M. Keck Foundation and NEDO. We acknowledge the support of the National Institute of Standards and Technology, U.S. Department of Commerce through grant 70NANB7H6177 and in providing neutron research facilities used in this work.

Received: October 9, 2010
Published online: March 22, 2011

[1] R. T Smith, GD Achenbac, R. Gerson, W. J. James, *J. Appl. Phys.* **1968**, *39*, 70.
[2] G. Smolenskii, I. Chupis, *Sov. Phys. Usp.* **1982** *25*, 475; Y. Venevtsev, V. Gagulin, *Ferroeletrics* **1994**, *162*, 23.
[3] T. Zhao, A. Scholl, F. Zavaliche, K. Lee, M. Barry, A. Doran, M. P. Cruz, Y. H. Chu, C. Ederr, N. A. Spaldin, R. R. Das, D. M. Kim, S. H. Baek, C. B. Eom, R. Ramesh, *Nat. Mater.* **2006**, *5*, 823.
[4] I. Sonowska, T. Peterlin-Neumaier, E. Steichele, *J. Phys. C.* **1982,** *15*, 4835; R. Przenioslo, M. Regulski, I. Sosnowska, *J. Phys. Soc. Jpn.* **2006**, *75*, 084718; S. Lee, T. Choi, W. Ratcliff II, R. Erwin, S-W. Cheong, V. Kiryukhin, *Phys. Rev. B* **2008**, *78*, 100101; D. Lebeugle, D. Colson, A. Forget, M. Viret, A. M. Bataille, A. Gukasov, *Phys. Rev. Lett.* **2008**, *100*, 227602; S. Lee, W. Ratcliff, S-W. Cheong, V. Kiryukhin, *Appl. Phys. Lett.* **2008**, *92*, 192906.
[5] H. Bea, M. Bibes, S. Petit, J. Kreisel, A. Barthelemy, *Philos. Mag. Lett* **2007**, *87*, 165.
[6] C. Ederer, N. A. Spaldin, *Phys. Rev. Lett.* **2005**, *71*, 060401.
[7] F. Bai, J. Wang, M. Wuttig, JieFang Li, Naigang Wang, A. P. Pyatakov, A. K. Zvezdin, L. E. Cross, D. Viehland, *Appl. Phys. Lett*. **2005**, *86*, 32511.
[8] D. Kan, I. Takeuchi, *J. Appl. Phys.* **2010**, *108*, 014104.
[9] D. H. Kim, H. N. Lee, M. D. Biegalski, H. M. Christen, *Appl. Phys. Lett.* **2008**, *92*, 012911.
[10] Y. H. Chu, T. Zhao, M. P. Cruz, Q. Zhan, P. L. Yang, L. W. Martin, M. Huijben, C. H. Yang, F. Zavaliche, H. Zheng, R. Ramesh, *Appl. Phys. Lett.* **2007**, *90*, 252906.
[11] G. Xu, J. Li, D. Viehland, *Appl. Phys. Lett.* **2006**, *89*, 222901.
[12] AI Zaslavskii, AG Tutov, *Doklady Akademii Nauk SSSR* **1960,** *135*, 815.
[13] J. Li, J. Wang, M. Wuttig, R. Ramesh, N. Wang, B. Ruette, A. P. Pyatakov, A. K. Zvezdin, D. Viehland, *Appl. Phys. Lett.* **2004**, *84,* 5261.
[14] J. W. Lynn, G. Shirane, M. Blume, *Phys. Rev. Lett.* **1976** *37*, 154.
[15] S. W. Lovesey, *Theory of Neutron Scattering from Condensed Matter* vol. *2* Oxford, New York, **1984**.
[16] W. Gavin Williams, *Polarized Neutrons,* Oxford, New York **1988**.
[17] Tapan Chatterji, *Neutron Scattering from Magnetic Materials,* Elsevier, Amsterdam, **2006**.
[18] D. Lebeugle, A. Mougin, M. Viret, D. Colson, L. Ranno. *Phys. Rev. Lett.* **2009**, *103*, 257601.
[19] Y.-H. Chu, L. W. Martin, M. B. Holcomb, M. Gajek, S.-J. Han, Q. He, N. Balke, C.-H. Yang, D. Lee, W. Hu, Q. Zhan, P.-L. Yang, A. Fraile-Rodríguez, A. Scholl, S. X. Wang, R. Ramesh, *Nat. Mater.* **2008**, *7*, 478–482.
[20] Any mention of commercial products within this paper is for information only; it does not imply recommendation or endorsement by NIST.
[21] W. C. Chen, R. Erwin, J. W. McIver, S. Watson, C. B. Fu, T. R. Gentile, J. A. Borchers, J. W. Lynn, G. L. Jones, *Physica B* **2009**, *404*, 2663.
[22] E. O. Wollan, W. C. Koehler, *Phys. Rev. B* **1955**, *100*, 545; David E. Cox, *IEEE Trans. Magn. 1972, 8,*161.